ISSN 0915-633X

# NATIONAL INSTITUTE FOR FUSION SCIENCE

## Axial and Equatorial Magnetic Dipoles Generated in a Rotating Spherical Shell

N. Ishihara and S. Kida

(Received - Mar. 8, 2000 )

NIFS-631 Mar. 2000



RESEARCH REPORT
NIFS Series

NAGOYA, JAPAN

# Axial and Equatorial Magnetic Dipoles Generated in a Rotating Spherical Shell

Norio ISHIHARA † and Shigeo KIDA

†*Department of Physics, Nagoya University, Nagoya, 464-8602*
*Theory and Computer Simulation Center, National Institute for Fusion Science, Toki, 509-5292*

Two types of magnetic dipole fields are generated by thermal convection in a rotating spherical shell. The axial (or equatorial) dipole in which the magnetic dipole moment is parallel (or perpendicular) to the rotation axis is realized at a larger (or smaller) value of the Rayleigh number. Their structure is robust and persists over the whole simulation period that is eight (or two) magnetic diffusion time.

KEYWORDS: dynamo, magnetic dipole, thermal convection, rotating spherical shell

Existence of the magnetic field in rotating spherical celestial bodies such as the Sun and planets has long been attracting scientific interests by offering such questions as how it is generated and why the dipole component is often dominant. Thermal convection of an electrically conducting fluid in celestial bodies is one of the most probable dynamo mechanisms. There are three essential elements for this convection dynamo to be realized, that is, rotation, spherical geometry, and convection (by nuclear reaction or phase transition).

As a simple model in which these elements are incorporated the thermally driven dynamo in a rotating spherical shell has been extensively studied by numerical simulation.[1-10] In this model a given temperature difference between the inner and outer spheres drives a convection of an electrically conducting fluid confined in a spherical shell rotating at constant angular velocity $\Omega$, which in turn intensifies the magnetic field. This is the dynamo action.

Different settings of simulations are devised depending on the purpose of dynamo research. Here, we make it in two steps.[5] First, starting with a slightly unstable thermal conduction state superimposed by random disturbances, we perform a purely non-magnetic simulation to get a fully developed thermal convection either of steady or unsteady state which is independent of the initial small disturbances. Then, a random weak magnetic field is seeded and its temporal evolution is investigated by a full MHD simulation. In this way we may elucidate the intensification mechanism of magnetic field by convection.[6]

There are five control parameters in the present system, which are the Rayleigh number $Ra$, the Taylor number $Ta$, the Roberts number $Ro$, the Prandtl number $Pr$, and the ratio $\eta$ of the radii of the outer and inner boundary spheres (see ref. 6 for definition). We are particularly interested in the phenomenon at large values of $Ra$ and $Ta$ as it is anticipated to be the case for the Sun and the Earth.

We have already reported a series of runs with $Ra = 3,200$ and $Ta = 8,000$, $Pr = 1$, $\eta = 0.5$, and changing values of $Ro$. The numerical simulation was performed by employing the Crank-Nicolson/ Adams-Bashforth scheme for time integration and the Chebyshev-Legendre-Fourier expansion for spatial resolution.[5-8] The thermal convection obtained is steady for these parameter values. An imposed weak magnetic field grows or decays according as $Ro$ is greater or smaller than a critical value 0.122. Amplitude of the resulting magnetic field gets larger as $Ro$ decreases. The magnetic energy is 2%, 30%, and 40% of the kinetic in the mean for $Ro = 0.12$, 0.1, and 0.07, respectively. The concentrate-and-stretch mechanism of the intensification of magnetic field was discovered for $Ro = 0.12$ where the magnetic field was not so strong as to alter the thermal convection. In all of these cases the magnetic dipole moment $\boldsymbol{m}(t) = \int \frac{1}{2}\boldsymbol{x} \times \boldsymbol{j}(\boldsymbol{x}, t)\mathrm{d}\boldsymbol{x}$, where $\boldsymbol{j}(\boldsymbol{x}, t)$ is the electric current density and the integration is carried out over the whole spherical shell, is dominated by the $z$-component (which is parallel to the rotation axis). It changes either periodically, quasi-periodically, or chaotically in time for $Ro = 0.12$, 0.10, or 0.07, respectively.

We describe here new results at a larger value of $Ta = 1.6 \times 10^6$, in which the energy of magnetic field exceeds that of convection field. The critical Rayleigh number $Ra_c$ of linear stability to a thermal conduction

†E-mail : ishihara@toki.theory.nifs.ac.jp

Table I. Parameters and flow characteristics. $(N, L, M)$ are the numbers of modes taken in the radial, latitudinal, and longitudinal directions, respectively. $Ta = 1.6 \times 10^6$. $Ra_c = 1.36 \times 10^4$.

| | Case I | Case II |
|---|---|---|
| Type of dipole field | equatorial | axial |
| Rayleigh number $Ra$ | $1.6 \times 10^4$ | $3.2 \times 10^4$ |
| Angular velocity of TP columns $\Omega_{TP}$ | 0.541 | $-0.9 \pm 0.08$ |
| Angular velocity of magnetic field $\Omega_{Mag}$ | 0.23 | —— |
| Number of TP columns | 6 | 9 |
| Roberts number $Ro$ | 0.02 | 0.1 |
| Critical Roberts number $Ro_c$ | 0.075 | 0.149 |
| Magnetic diffusion time $d^2/\lambda$ | 50 | 10 |
| Viscous diffusion time $d^2/\nu$ | 1 | 1 |
| Thermal diffusion time $d^2/\kappa$ | 1 | 1 |
| Resolution $(N, L, M)$ | $(64, 64, 128)$ | $(128, 64, 128)$ |
| Time step width $\Delta t$ | $2.5 \times 10^{-4}$ | $1.25 \times 10^{-5}$ |

state at this Taylor number is then found to be $Ra_c = 1.36 \times 10^4$ (see Table I). We choose a slightly unstable Rayleigh number $Ra = 1.6 \times 10^4$ (Case I) and the double $3.2 \times 10^4$ (Case II) of it. In Case I, six pairs of cyclonic and anti-cyclonic Taylor-Proudman (TP) vortex columns emerge, which are unsteady and prograde with mean angular velocity $\Omega_{TP} = 0.541$, where time is normalized by the thermal diffusion time. In Case II, on the other hand, nine pairs of vortex columns appear which vary in time more violently and retrograde with mean angular velocity $\Omega_{TP} = -0.9 \pm 0.08$. These angular velocities are much smaller than that of the rotating shell itself $\Omega \approx 632$.

A random weak magnetic field is seeded in these thermal convection flows. The critical Roberts number $Ro_c$ which divides the growth and decay of magnetic field is about 0.075 for Case I and 0.149 for Case II. In the following we present simulation results for $Ro = 0.02$ (Case I) and $Ro = 0.1$ (Case II). Incidentally, the spectrum of the dependent variables in the Chebyshev-Legendre-Fourier expansion decays at large wavenumbers rapidly enough to ensure the numerical accuracy.

In the both cases the amplitude of magnetic field begins to increase exponentially in time and keeps growing until the magnetic and velocity fields become comparable in magnitude. After this time the two fields fluctuate irregularly around statistically equilibrium states.

In Fig. 1, we show a snapshot of magnetic field in the equilibrium period for Case I. The magnetic lines plotted outside the outer sphere are seen from a high latitude of the Northern hemisphere in the top panel, where color of the lines indicates the direction of the magnetic field which is pointed from red to blue. They form a dipole structure, the axis of the dipole moment of which lies on the equatorial plane and rotates around the rotation axis of the spherical shell. The angular velocity 0.23 (cf. Fig. 3(a)) is about a half of that of Taylor-Proudman columns. The pattern of the magnetic field lines in the equatorial plane is shown in the bottom panel with many lines, the length of which is proportional to the strength and a circle at an edge denotes the direction of the magnetic field pointed to. Color map on the annulus indicates magnitude of the magnetic field (stronger for red and weaker for blue), the equatorial ($x$ and $y$) component of which is overwhelming. At the same time the axial ($z$) component of vorticity is drawn with white and black contours for $\omega_z < 0$ (anti-cyclones) and $\omega_z > 0$ (cyclones), respectively. Strong magnetic field is localized in the neighborhood of a couple of anti-cyclones which locate symmetrically with respect to the origin. It is interesting to note that the six-fold symmetric around the origin (see white and black contours) still remains in the convection field, whereas the symmetry of magnetic field is only two-fold. Such a coexistence of different symmetries was also observed at other parameters.[6] These intensified regions of magnetic field retrogrades relative to the convection field (see below). Magnetic lines are running along streamlines (not shown) in the frame in which convection field is steady.

In Fig. 2, we plot an instantaneous structure of the magnetic field in the equilibrium period for Case II. It is seen that strong magnetic flux density is localized in some particular areas. The axial component is dominant inside a couple of anti-cyclones, whereas the equatorial component is intensified between neighboring cyclones and anti-cyclones. In the same way as Case I, strong magnetic lines are along streamlines (not shown). Notice that all of these strong magnetic field is being intensified by the concentrate-and-stretch mechanism[6] in the places where flows come out of thin boundary layers, that is, the stagnation points on the equatorial plane, on the outer boundary, or on the inner boundary.

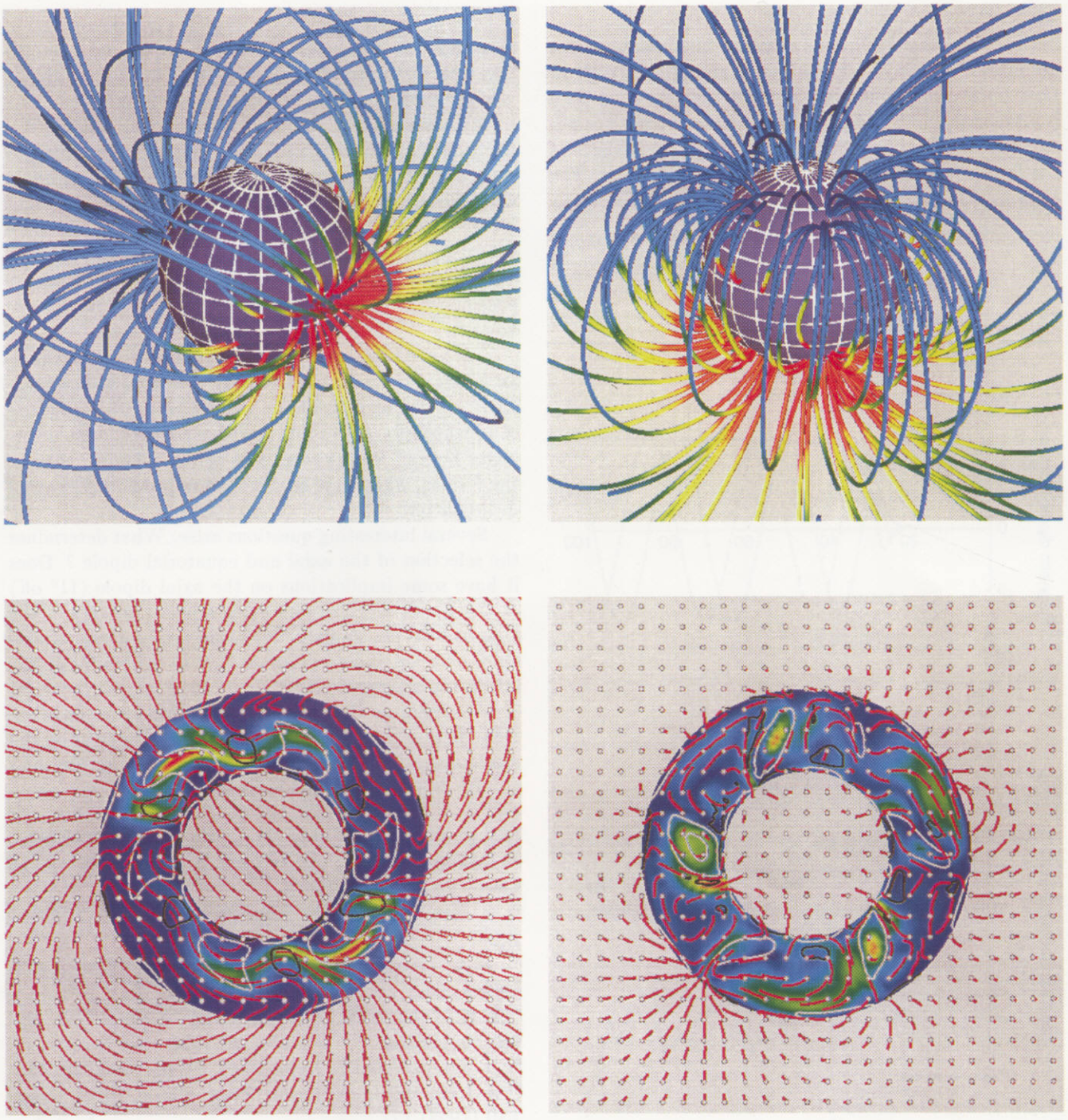

Figure 1 (left panel). Equatorial magnetic dipole. Top: Magnetic lines which are pointed from red to blue. They are drawn by numerical integration starting from the outer sphere. The number density of the starting points varies depending on the magnitude of $B_r$ the radial component of the magnetic field on the surface. They are distributed on $32 \times 64$ points in the $\theta$- and $\phi$- directions for $|B_r| \geq 2$, $16 \times 32$ for $1 \leq |B_r| < 2$, $8 \times 16$ for $0.5 \leq |B_r| < 1$, $4 \times 8$ for $0.25 \leq |B_r| < 0.5$, and $2 \times 4$ for $|B_r| < 0.25$. $-4.1 \leq B_r \leq 2.8$. Bottom: Structure of the magnetic and vorticity fields on the equatorial plane. Color map represents the magnitude of the magnetic field which is stronger for red and weaker for blue. The magnetic lines in the equatorial plane are shown by red lines with circles to which the magnetic field is directed. The axial component of vorticity is drawn with white and black contours for anti-cyclones and cyclones, respectively. $t = 100$.
Figure 2 (right panel). Axial magnetic dipole. The quantities plotted are the same as in Fig. 1. The starting points of the magnetic lines are distributed on $32 \times 64$ points in the $\theta$- and $\phi$- directions for $|B_r| \geq 16$, $16 \times 32$ for $8 \leq |B_r| < 16$, $8 \times 16$ for $4 \leq |B_r| < 8$, and $4 \times 8$ for $|B_r| < 4$. $-23.7 \leq B_r \leq 23.2$. $t = 60$.

The temporal evolutions of magnetic dipole moment are shown in Fig. 3 for (a) Case I and (b) Case II. In Case I, the dashed and dotted lines denote the equatorial components which oscillate in time after a transient period $t \gtrsim 30$. The phase of the former is $90^o$ in advance of the latter. The axial component is invisibly small. The solid line represents the magnitude $\sqrt{m_x^2 + m_y^2}$ of the equatorial component which increases slowly in time.

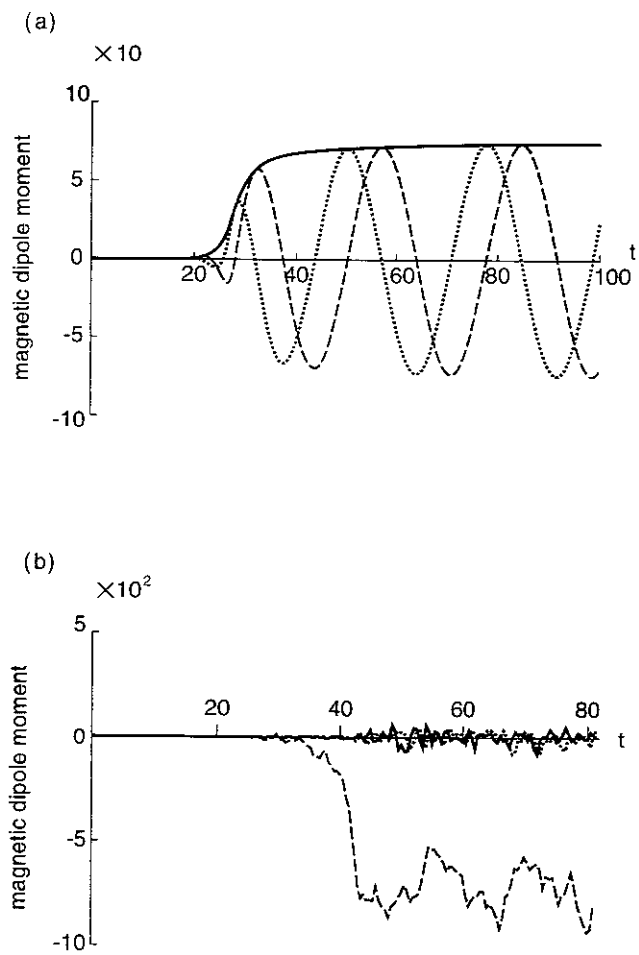


Figure 3. Temporal evolution of magnetic dipole moment. (a) Case I. $m_x$, dashed line; $m_y$, dotted line; $\sqrt{m_x^2 + m_y^2}$, solid line. (b) Case II. $m_x$, solid line; $m_y$, dotted line; $m_z$, dashed line. The magnetic dipole moment is normalized by $\kappa(\mu\rho)^{1/2}d^2$, and the time by $d^2/\kappa$, where $\kappa$ is the thermal diffusivity, $\mu$ the magnetic permeability, $\rho$ the fluid density, $d$ the thickness of the spherical shell.

Therefore the dipole vector retrogrades around the rotation axis in the equatorial plane with constant angular velocity 0.23 (found by reading on the graph).

By contrast, in Case II, after a transient time $t \gtrsim 42$, the axial component dominates the equatorial component so that the magnetic dipole moment aligns almost with the rotation axis. The deviation angle is less than $9^o$. The magnitude of the axial component varies in time substantially but the sign never changes during the simulation period (over eight magnetic diffusion time). A possibility of reversal at later times cannot be denied, however.

We have seen two types of magnetic dipole fields in an MHD simulation of a rotating spherical shell model. They are the equatorial and axial dipoles, the structure of which is robust and rotate with a constant angular velocity around the rotation axis of the spherical shell in the former, whereas it does not show a polarity reversal in the latter.

Several interesting questions arise. What determines the selection of the axial and equatorial dipole ? Does it have some implications on the axial dipole ($11^o$ off) of the Earth and the non-axial dipole ($59^o$ off) of the Uranus ? What happens for a range of control parameters between these two cases ? Will equatorial or axial dipole emerge ? How about the magnetic reversal ?[5,8,11] What on Earth is the intensification mechanism ? Studies on these interesting problems as well as on the mechanism of each dipole field are now under way and will be discussed in a forthcoming paper.


[1] F.H. Busse: Ann. Rev. Fluid Mech. **10** (1978) 435.
[2] P.H. Roberts and A.M. Soward: Annu. Rev. Fluid Mech. **24** (1992) 459.
[3] A. Kageyama and T. Sato: Phys. Plasmas **2** (1995) 1421.
[4] G.A. Glatzmaier and P.H. Roberts: Nature **377** (1995) 203.
[5] S. Kida, K. Araki and H. Kitauchi: J. Phys. Soc. Jpn **66** (1997) 2194.
[6] H. Kitauchi and S. Kida: Phys. Fluids **10** (1998) 457.
[7] S. Kida and H. Kitauchi: Prog. Theor. Phys. Supp. **130** (1998) 121.
[8] S. Kida and H. Kitauchi: J. Phys. Soc. Jpn **67** (1998) 2950.
[9] H. Kitauchi, K. Araki and S. Kida: Nonlinearity **10** (1997) 885.
[10] A. Sakuraba and M. Kono: Phys. Earth. Planet. Inter. **111** (1999) 105.
[11] G.A. Glatzmaier, R.S. Coe, L. Hongre and P.H. Roberts: Nature **401** (1999) 885.

## Recent Issues of NIFS Series

NIFS-566 N. Nakajima, J. Chen, K. Ichiguchi and M. Okamoto,
*Global Mode Analysis of Ideal MHD Modes in L=2 Heliotron/Torsatron Systems*, Oct 1998
(IAEA-CN-69/THP1/08)

NIFS-567 K. Ida, M. Osakabe, K. Tanaka, T. Minami, S. Nishimura, S. Okamura, A. Fujisawa, Y. Yoshimura, S. Kubo, R. Akiyama, D.S. Darrow, H. Idei, H. Iguchi, M. Isobe, S. Kado, T. Kondo, S. Lee, K. Matsuoka, S. Morita, I. Nomura, S. Ohdachi, M. Sasao, A. Shimizu, K. Tumori, S. Takayama, M. Takechi, S. Takagi, C. Takahashi, K. Toi and T. Watari,
*Transition from L Mode to High Ion Temperature Mode in CHS Heliotron/Torsatron Plasmas*; Oct 1998
(IAEA-CN-69/EX2/2)

NIFS-568 S. Okamura, K. Matsuoka, R. Akiyama, D.S. Darrow, A. Ejiri, A. Fujisawa, M. Fujiwara, M. Goto, K. Ida, H. Idei, H. Iguchi, N. Inoue, M. Isobe, K. Itoh, S. Kado, K. Khlopenkov, T. Kondo, S. Kubo, A. Lazaros, S. Lee, G. Matsunaga, T. Minami, S. Morita, S. Murakami, N. Nakajima, N. Nikai, S. Nishimura, I. Nomura, S. Ohdachi, K. Ohkuni, M. Osakabe, R. Pavlichenko, B. Peterson, R. Sakamoto, H. Sanuki, M. Sasao, A. Shimizu, Y. Shirai, S. Sudo, S. Takagi, C. Takahashi, S. Takayama, M. Takechi, K. Tanaka, K. Toi, K. Yamazaki, Y. Yoshimura and T. Watari,
*Confinement Physics Study in a Small Low-Aspect-Ratio Helical Device CHS*, Oct 1998
(IAEA-CN-69/OV4/5)

NIFS-569 M.M. Skoric, T. Sato, A. Maluckov, M.S. Jovanovic,
*Micro- and Macro-scale Self-organization in a Dissipative Plasma*, Oct. 1998

NIFS-570 T. Hayashi, N. Mizuguchi, T-H. Watanabe, T. Sato and the Complexity Simulation Group,
*Nonlinear Simulations of Internal Reconnection Event in Spherical Tokamak*; Oct 1998
(IAEA-CN-69/TH3/3)

NIFS-571 A. Iiyoshi, A. Komori, A. Ejiri, M. Emoto, H. Funaba, M. Goto, K. Ida, H. Idei, S. Inagaki, S. Kado, O. Kaneko, K. Kawahata, S. Kubo, R. Kumazawa, S. Masuzaki, T. Minami, J. Miyazawa, T. Morisaki, S. Morita, S. Murakami, S. Muto, T. Muto, Y. Nagayama, Y. Nakamura, H. Nakanishi, K. Narihara, K. Nishimura, N. Noda, T. Kobuchi, S. Ohdachi, N. Ohyabu, Y. Oka, M. Osakabe, T. Ozaki, B.J. Peterson, A. Sagara, S. Sakakibara, R. Sakamoto, H. Sasao, M. Sasao, K. Sato, M. Sato, T. Seki, T. Shimozuma, M. Shoji, H. Suzuki, Y. Takeiri, K. Tanaka, K. Toi, T. Tokuzawa, K. Tsumori, I. Yamada, H. Yamada, S. Yamaguchi, M. Yokoyama, K.Y. Watanabe, T. Watari, R. Akiyama, H. Chikaraishi, K. Haba, S. Hamaguchi, S. Iima, S. Imagawa, N. Inoue, K. Iwamoto, S. Kitagawa, Y. Kubota, J. Kodaira, R. Maekawa, T. Mito, T. Nagasaka, A. Nishimura, Y. Takita, C. Takahashi, K. Takahata, K. Yamauchi, H. Tamura, T. Tsuzuki, S. Yamada, N. Yanagi, H. Yonezu, Y. Hamada, K. Matsuoka, K. Murai, K. Ohkubo, I. Ohtake, M. Okamoto, S. Sato, T. Satow, S. Sudo, S. Tanahashi, K. Yamazaki, M. Fujiwara and O. Motojima,
*An Overview of the Large Helical Device Project*, Oct. 1998
(IAEA-CN-69/OV1/4)

NIFS-572 M. Fujiwara, H. Yamada, A. Ejiri, M. Emoto, H. Funaba, M. Goto, K. Ida, H. Idei, S. Inagaki, S. Kado, O. Kaneko, K. Kawahata, A. Komori, S. Kubo, R. Kumazawa, S. Masuzaki, T. Minami, J. Miyazawa, T. Morisaki, S. Morita, S. Murakami, S. Muto, T. Muto, Y. Nagayama, Y. Nakamura, H. Nakanishi, K. Narihara, K. Nishimura, N. Noda, T. Kobuchi, S. Ohdachi, N. Ohyabu, Y. Oka, M. Osakabe, T. Ozaki, B. J. Peterson, A. Sagara, S. Sakakibara, R. Sakamoto, H. Sasao, M. Sasao, K. Sato, M. Sato, T. Seki, T. Shimozuma, M. Shoji, H. Sazuki, Y. Takeiri, K. Tanaka, K. Toi, T. Tokuzawa, K. Tsumori, I. Yamada, S. Yamaguchi, M. Yokoyama, K.Y. Watanabe, T. Watari, R. Akiyama, H. Chikaraishi, K. Haba, S. Hamaguchi, M. Iima, S. Imagawa, N. Inoue, K. Iwamoto, S. Kitagawa, Y. Kubota, J. Kodaira, R. Maekawa, T. Mito, T. Nagasaka, A. Nishimura, Y. Takita, C. Takahashi, K. Takahata, K. Yamauchi, H. Tamura, T. Tsuzuki, S. Yamada, N. Yanagi, H. Yonezu, Y. Hamada, K. Matsuoka, K. Murai, K. Ohkubo, I. Ohtake, M. Okamoto, S. Sato, T. Satow, S. Sudo, S. Tanahashi, K. Yamazaki, O. Motojima and A. Iiyoshi,
*Plasma Confinement Studies in LHD;* Oct. 1998
(IAEA-CN-69/EX2/3)

NIFS-573 O. Motojima, K. Akaishi, H. Chikaraishi, H. Funaba, S. Hamaguchi, S. Imagawa, S. Inagaki, N. Inoue, A. Iwamoto, S. Kitagawa, A. Komori, Y. Kubota, R. Maekawa, S. Masuzaki, T. Mito, J. Miyazawa, T. Morisaki, T. Muroga, T. Nagasaka, Y. Nakmura, A. Nishimura, K. Nishimura, N. Noda, N. Ohyabu, S. Sagara, S. Sakakibara, R. Sakamoto, S. Satoh, T. Satow, M. Shoji, H. Suzuki, K. Takahata, H. Tamura, K. Watanabe, H. Yamada, S. Yamada, S. Yamaguchi, K. Yamazaki, N. Yanagi, T. Baba, H. Hayashi, M. Iima, T. Inoue, S. Kato, T. Kato, T. Kondo, S. Moriuchi, H. Ogawa, I. Ohtake, K. Ooba, H. Sekiguchi, N. Suzuki, S. Takami, Y. Taniguchi, T. Tsuzuki, N. Yamamoto, K. Yasui, H. Yonezu, M. Fujiwara and A. Iiyoshi,
*Progress Summary of LHD Engineering Design and Construction*, Oct 1998
(IAEA-CN-69/FT2/1)

NIFS-574 K. Toi, M. Takechi, S. Takagi, G. Matsunaga, M. Isobe, T. Kondo, M. Sasao, D.S. Darrow, K. Ohkuni, S. Ohdachi, R. Akiyama, A. Fujisawa, M. Gotoh, H. Idei, K. Ida, H. Iguchi, S. Kado, M. Kojima, S. Kubo, S. Lee, K. Matsuoka, T. Minami, S. Morita, N. Nikai, S. Nishimura, S. Okamura, M. Osakabe, A. Shimizu, Y. Shirai, C. Takahashi, K. Tanaka, T. Watari and Y. Yoshimura,
*Global MHD Modes Excited by Energetic Ions in Heliotron/Torsatron Plasmas*; Oct 1998
(IAEA-CN-69/EXP1/19)

NIFS-575 Y. Hamada, A. Nishizawa, Y. Kawasumi, A. Fujisawa, M. Kojima, K. Narihara, K. Ida, A. Ejiri, S. Ohdachi, K. Kawahata, K. Toi, K. Sato, T. Seki, H. Iguchi, K. Adachi, S. Hidekuma, S. Hirokura, K. Iwasaki, T. Ido, R. Kumazawa, H. Kuramoto, T. Minami, I. Nomura, M. Sasao, K.N. Sato, T. Tsuzuki, I. Yamada and T. Watari,
*Potential Turbulence in Tokamak Plasmas*; Oct 1998
(IAEA-CN-69/EXP2/14)

NIFS-576 S. Murakami, U. Gasparino, H. Idei, S. Kubo, H. Maassberg, N. Marushchenko, N. Nakajima, M. Romé and M. Okamoto,

*5D Simulation Study of Suprathermal Electron Transport in Non-Axisymmetric Plasmas*;Oct. 1998 (IAEA-CN-69/THP1/01)

NIFS-577 S. Fujiwara and T Sato,
*Molecular Dynamics Simulation of Structure Formation of Short Chain Molecules*; Nov 1998

NIFS-578 T. Yamagishi,
*Eigenfunctions for Vlasov Equation in Multi-species Plasmas* Nov. 1998

NIFS-579 M. Tanaka, A Yu Grosberg and T. Tanaka,
*Molecular Dynamics of Strongly-Coupled Multichain Coulomb Polymers in Pure and Salt Aqueous Solutions*, Nov. 1998

NIFS-580 J. Chen, N. Nakajima and M Okamoto,
*Global Mode Analysis of Ideal MHD Modes in a Heliotron/Torsatron System: I Mercier-unstable Equilibria*, Dec 1998

NIFS-581 M. Tanaka, A Yu Grosberg and T. Tanaka,
*Comparison of Multichain Coulomb Polymers in Isolated and Periodic Systems: Molecular Dynamics Study;* Jan. 1999

NIFS-582 V.S. Chan and S. Murakami,
*Self-Consistent Electric Field Effect on Electron Transport of ECH Plasmas*, Feb. 1999

NIFS-583 M Yokoyama, N. Nakajima, M. Okamoto, Y Nakamura and M. Wakatani,
*Roles of Bumpy Field on Collisionless Particle Confinement in Helical-Axis Heliotrons*; Feb. 1999

NIFS-584 T-H Watanabe, T. Hayashi, T. Sato, M. Yamada and H Ji,
*Modeling of Magnetic Island Formation in Magnetic Reconnection Experiment*, Feb 1999

NIFS-585 R. Kumazawa, T. Mutoh, T Seki, F. Shinpo, G. Nomura, T. Ido, T Watari, Jean-Marie Noterdaeme and Yangping Zhao,
*Liquid Stub Tuner for Ion Cyclotron Heating*; Mar. 1999

NIFS-586 A. Sagara, M. Iima, S. Inagaki, N. Inoue, H. Suzuki, K. Tsuzuki, S. Masuzaki, J. Miyazawa, S. Morita, Y Nakamura, N. Noda, B Peterson, S. Sakakibara, T. Shimozuma, H. Yamada, K. Akaishi, H. Chikaraishi, H. Funaba, O. Kaneko, K. Kawahata, A. Komori, N Ohyabu, O Motojima, LHD Exp. Group 1, LHD Exp. Group 2,
*Wall Conditioning at the Starting Phase of LHD*; Mar. 1999

NIFS-587 T Nakamura and T. Yabe,
*Cubic Interpolated Propagation Scheme for Solving the Hyper-Dimensional Vlasov-Poisson Equation in Phase Space*; Mar. 1999

NIFS-588 W.X. Wnag, N. Nakajima, S. Murakami and M. Okamoto,
*An Accurate δf Method for Neoclassical Transport Calculation*; Mar. 1999

NIFS-589 K. Kishida, K. Araki, S. Kishiba and K. Suzuki,
*Local or Nonlocal? Orthonormal Divergence-free Wavelet Analysis of Nonlinear Interactions in Turbulence*; Mar 1999

NIFS-590 K. Araki, K. Suzuki, K. Kishida and S. Kishiba,
*Multiresolution Approximation of the Vector Fields on $T^3$*; Mar. 1999

NIFS-591 K. Yamazaki, H. Yamada, K.Y Watanabe, K. Nishimura, S. Yamaguchi, H. Nakanishi, A. Komori, H. Suzuki, T Mito, H. Chikaraishi, K. Murai, O. Motojima and the LHD Group,
*Overview of the Large Helical Device (LHD) Control System and Its First Operation*; Apr. 1999

NIFS-592 T. Takahashi and Y Nakao,
*Thermonuclear Reactivity of D-T Fusion Plasma with Spin-Polarized Fuel*; Apr. 1999

NIFS-593 H. Sugama,
*Damping of Toroidal Ion Temperature Gradient Modes*; Apr. 1999

NIFS-594 Xiaodong Li,
*Analysis of Crowbar Action of High Voltage DC Power Supply in the LHD ICRF System*; Apr. 1999

NIFS-595 K. Nishimura, R. Horiuchi and T. Sato,

*Drift-kink Instability Induced by Beam Ions in Field-reversed Configurations*, Apr 1999

NIFS-596 Y Suzuki, T-H Watanabe, T Sato and T Hayashi,
*Three-dimensional Simulation Study of Compact Toroid Plasmoid Injection into Magnetized Plasmas*; Apr 1999

NIFS-597 H Sanuki, K Itoh, M. Yokoyama, A Fujisawa, K Ida, S Toda, S-I Itoh, M Yagi and A Fukuyama,
*Possibility of Internal Transport Barrier Formation and Electric Field Bifurcation in LHD Plasma*, May 1999

NIFS-598 S Nakazawa, N. Nakajima, M Okamoto and N Ohyabu,
*One Dimensional Simulation on Stability of Detached Plasma in a Tokamak Divertor*, June 1999

NIFS-599 S Murakami, N. Nakajima, M. Okamoto and J. Nhrenberg,
*Effect of Energetic Ion Loss on ICRF Heating Efficiency and Energy Confinement Time in Heliotrons*, June 1999

NIFS-600 R Horiuchi and T. Sato,
*Three-Dimensional Particle Simulation of Plasma Instabilities and Collisionless Reconnection in a Current Sheet*;, June 1999

NIFS-601 W Wang, M Okamoto, N Nakajima and S Murakami,
*Collisional Transport in a Plasma with Steep Gradients*, June 1999

NIFS-602 T Mutoh, R Kumazawa, T. Saki, K Saito, F. Simpo, G Nomura, T Watari, X Jikang, G Cattanei, H Okada, K Ohkubo, M. Sato, S Kubo, T. Shimozuma, H Idei, Y Yoshimura, O. Kaneko, Y Takeiri, M. Osakabe, Y Oka, K Tsumori, A Komori, H. Yamada, K Watanabe, S Sakakibara, M Shoji, R Sakamoto, S Inagaki, J Miyazawa, S Morita, K Tanaka, B.J. Peterson, S Murakami, T Minami, S Ohdachi, S Kado, K Narihara, H Sasao, H Suzuki, K Kawahata, N Ohyabu, Y. Nakamura, H Funaba, S Masuzaki, S Muto, K Sato, T Morisaki, S Sudo, Y Nagayama, T Watanabe, M Sasao, K. Ida, N Noda, K Yamazaki, K Akaishi, A Sagara, K Nishimura, T. Ozaki, K Toi, O Motojima, M Fujiwara, A Iiyoshi and LHD Exp Group 1 and 2,
*First ICRF Heating Experiment in the Large Helical Device*: July 1999

NIFS-603 P C. de Vries, Y Nagayama, K Kawahata, S Inagaki, H Sasao and K Nagasaki,
*Polarization of Electron Cyclotron Emission Spectra in LHD*, July 1999

NIFS-604 W. Wang, N. Nakajima, M. Okamoto and S Murakami,
*δf Simulation of Ion Neoclassical Transport;* July 1999

NIFS-605 T. Hayashi, N. Mizuguchi, T Sato and the Complexity Simulation Group,
*Numerical Simulation of Internal Reconnection Event in Spherical Tokamak*; July 1999

NIFS-606 M. Okamoto, N Nakajima and W Wang,
*On the Two Weighting Scheme for δf Collisional Transport Simulation*, Aug. 1999

NIFS-607 O. Motojima, A.A. Shishkin, S. Inagaki, K.Y Watanabe,
*Possible Control Scenario of Radial Electric Field by Loss-Cone-Particle Injection into Helical Device*, Aug 1999

NIFS-608 R Tanaka, T. Nakamura and T. Yabe,
*Constructing Exactly Conservative Scheme in Non-conservative Form*, Aug 1999

NIFS-609 H Sugama,
*Gyrokinetic Field Theory*, Aug 1999

NIFS-610 M. Takechi, G Matsunaga, S Takagi, K Ohkuni, K Toi, M Osakabe, M Isobe, S. Okamura, K Matsuoka, A Fujisawa, H. Iguchi, S Lee, T Minami, K Tanaka, Y Yoshimura and CHS Group,
*Core Localized Toroidal Alfven Eigenmodes Destabilized By Energetic Ions in the CHS Heliotron/Torsatron*; Sep. 1999

NIFS-611 K Ichiguchi,
*MHD Equilibrium and Stability in Heliotron Plasmas*; Sep 1999

NIFS-612 Y Sato, M. Yokoyama, M. Wakatani and V D Pusovitov,
*Complete Suppression of Pfirsch-Schluter Current in a Toroidal l=3 Stellarator*, Oct. 1999

NIFS-613 S. Wang, H. Sanuki and H. Sugama,

*Reduced Drift Kinetic Equation for Neoclassical Transport of Helical Plasmas in Ultra-low Collisionality Regime*;Oct. 1999

NIFS-614 J. Miyazawa, H. Yamada, K. Yasui, S. Kato, N., Fukumoto, M. Nagata and T. Uyama,
*Design of Spheromak Injector Using Conical Accelerator for Large Helical Device*;Nov. 1999

NIFS-615 M. Uchida, A. Fukuyama, K. Itoh, S.-I. Itoh and M. Yagi,
*Analysis of Current Diffusive Ballooning Mode in Tokamaks*; Dec. 1999

NIFS-616 M. Tanaka, A.Yu Grosberg and T Tanaka,
*Condensation and Swelling Behavior of Randomly Charged Multichain Polymers by Molecular Dynamics Simulations;* Dec. 1999

NIFS-617 S. Goto and S. Kida,
*Sparseness of Nonlinear Coupling*; Dec. 1999

NIFS-618 M.M. Skoric, T. Sato, A. Maluckov and M.S. Jovanovic,
*Complexity in Laser Plasma Instabilities* Dec. 1999

NIFS-619 T.-H. Watanabe, H. Sugama and T. Sato,
*Non-dissipative Kinetic Simulation and Analytical Solution of Three-mode Equations of Ion Temperature Gradient Instability*; Dec. 1999

NIFS-620 Y. Oka, Y. Takeiri, Yu.I.Belchenko, M. Hamabe, O. Kaneko, K. Tsumori, M. Osakabe, E. Asano, T. Kawamoto, R. Akiyama,
*Optimization of Cs Deposition in the 1/3 Scale Hydrogen Negative Ion Source for LHD-NBI System* ,Dec. 1999

NIFS-621 Yu.I. Belchenko, Y Oka, O Kaneko, Y. Takeiri, A. Krivenko, M. Osakabe, K Tsumori, E. Asano, T. Kawamoto, R. Akiyama,
*Recovery of Cesium in the Hydrogen Negative Ion Sources*;Dec. 1999

NIFS-622 Y. Oka, O. Kaneko, K. Tsumori, Y. Takeiri, M. Osakabe, T. Kawamoto, E. Asano, and R. Akiyama,
*H- Ion Source Using a Localized Virtual Magnetic Filter in the Plasma Electrode: Type I LV Magnetic Filter:* Dec. 1999

NIFS-623 M. Tanaka, S Kida, S. Yanase and G. Kawahara,
*Zero-absolute-vorticity State in a Rotating Turbulent Shear Flow*;Jan. 2000

NIFS-624 F. Leuterer, S. Kubo,
*Electron Cyclotron Current Drive at $\omega \approx \omega_c$ with X-mode Launched from the Low Field Side;* Feb. 2000

NIFS-625 K. Nishimura,
*Wakefield of a Charged Particulate Influenced by Emission Process of Secondary Electrons*;Mar. 2000

NIFS-626 K. Itoh, M. Yagi, S.-I. Itoh, A. Fukuyama,
*On Turbulent Transport in Burning Plasmas*;Mar. 2000

NIFS-627 K. Itoh, S.-I. Itoh, L. Giannone,
*Modelling of Density Limit Phenomena in Toroidal Helical Plasmas*; Mar 2000

NIFS-628 K. Akaishi, M. Nakasuga and Y. Funato,
*True and Measured Outgassing Rates of a Vacuum Chamber with a Reversibly Absorbed Phase*;Mar. 2000

NIFS-629 T. Yamagishi,
*Effect of Weak Dissipation on a Drift Orbit Mapping*; Mar. 2000

NIFS-630 S. Toda, S.-I, Itoh, M. Yagi, A. Fukuyama and K. Itoh,
*Spatial Structure of Compound Dither in L/H Transition*;Mar. 2000

NIFS-631 N. Ishihara and S. Kida,
*Axial and Equatorial Magnetic Dipoles Generated in a Rotating Spherical Shell;* Mar. 2000